

Salicylic acid primed defence response in octoploid strawberry (Benihoppe) leaves induces resistance against *Podosphaera aphanis* through enhanced accumulation of proanthocyanidins and up-regulation of pathogenesis-related genes

Jun Feng

Beijing Forestry University

Min Zhang

Beijing Forestry University

Kangning Yang

Beijing Forestry University

Wenting You

Shanxi University

Caixia Zheng (✉ zhengcx@bjfu.edu.cn)

Beijing Forestry University <https://orcid.org/0000-0003-0142-4481>

Research article

Keywords: Salicylic acid-primed defence, response in octoploid strawberry, (Benihoppe)

Posted Date: October 30th, 2019

DOI: <https://doi.org/10.21203/rs.2.16580/v1>

License:  This work is licensed under a Creative Commons Attribution 4.0 International License.

[Read Full License](#)

Version of Record: A version of this preprint was published at BMC Plant Biology on April 8th, 2020. See the published version at <https://doi.org/10.1186/s12870-020-02353-z>.

Abstract

Background *Podosphaera aphanis*, a predominately biotrophic fungal pathogen, causes significant yield losses of strawberry. China is the largest strawberry producer in the world, and selecting for powdery mildew-resistant cultivars is desirable. However, the resistance mechanism against *P. aphanis* in the octoploid strawberry remains unclear.

Results To understand the molecular resistance mechanisms, we inoculated strawberry with *P. aphanis*, and examined the expression profiles of candidate genes and the biochemical phenotypes in strawberry leaves of two groups. The unigenes obtained from salicylic acid (SA)-untreated (SA⁻) and treated (SA⁺) leaves resulted in a total of 48,020 and 45,896 genes, respectively. KEGG enrichment showed that phenylpropanoid biosynthesis, plant–pathogen interaction, and plant hormone signal transduction pathways were enriched to a noticeable extent. Comparative analysis demonstrated that genes associated with the SA signalling pathway were significantly upregulated in the strawberry–*P. aphanis* interaction. In particular, the genes *FaTGA*, *FaDELLA*, and *FaJAZ* negatively regulating salicylic acid SA-responsive genes, whereas *FaNPR1*, *FaWRKY33*, *FaWRKY70*, and *FaMYC2* positively regulated SA-responsive genes, leading to increased expression of SA-responsive genes compared to a significant decline in expression of jasmonic acid-responsive genes.

Conclusions This study describes the role of total flavonoid content, proanthocyanidins (PAs), pathogenesis-related (PR) proteins, SA, and transcription factors in regulatory model against *P. aphanis*, which coincided with an early activation of defence, leading to the accumulation of PAs and the production of PR proteins.

Background

Plants have evolved immune systems to defend against various pathogenic microorganisms, which rely on the recognition of potential effectors by both pathogen-associated molecular pattern-triggered and effector-triggered immunity [1]; the defence mechanisms include oxidative burst, reinforcement of the cell wall, production of pathogenesis-related (PR) proteins, and a rapid hypersensitive response (HR) at the penetration site [2]. Powdery mildew (PM) is a widespread fungal disease of most plants, caused by Ascomycetes [3], which are obligate biotrophic fungi that form haustoria for the uptake of nutrient. Over 400 PM species colonise nearly 10,000 angiosperm species [4], including monocotyledonous and dicotyledonous plants [5]. Previous plant PM research has focused on major resistance genes involved in signalling pathways and secondary metabolites, especially in economically important crops, such as tomato, barley, apple, and wheat, as well as in the reference species *Arabidopsis* [6]. Therefore, the study of molecular resistance mechanisms is vital to improve the quality and yield of economically important crops.

Emerging evidence has shown that phytohormones, especially salicylic acid (SA) and jasmonic acid (JA), and ethylene (ET) signalling pathways regulate plant defence against various pathogens [7]. Upon

biotrophic pathogen attack, the accumulation of endogenous SA induces expression of several PR genes to enhance resistance. The SA- and JA/ET-mediated defence pathways are often mutually antagonistic [8]. When SA levels increase, NPR1 oligomers dissociate into monomers, which then enter the nucleus and interact with TGA transcription factors (TFs) [9] and TGA-interacting GLUTAREDOXIN 480 (GRX480), which regulates SA/JA antagonism [10]. WRKY70 is also required for expression of pathogenesis-related protein (PR1) and is a key regulator of SA/JA antagonism [11]. In *Arabidopsis*, SA-mediated defence plays a vital role against biotrophs, while JA/ET defends against necrotrophs [12]. Orthologues of genes involved in SA–JA crosstalk include NPR1, WRKY70, GRX480, MYC2, and JAZs [13]. SA/JA pathway antagonism interacts with other phytohormones (such as ET and gibberellic acid), regulating trade-offs between biotrophs and necrotrophs.

The PM *Podosphaera aphanis* is a biotrophic fungal disease of strawberry [14] that results in considerable losses in production and is deemed to be one of the most destructive diseases. The octoploid strawberry (*Fragaria × ananassa*) is a perennial plant with asexual stolon reproduction belonging to *Rosaceae* [15]; this commercially crop is widely cultivated in China. Due to the large-scale promotion of Japanese varieties (especially Benihoppe and new varieties derived from Benihoppe) and suitable environmental conditions in winter greenhouses, *P. aphanis* has become serious disease in China [16]. Despite the availability of total genome sequence information for octoploid strawberry [17], its mechanisms of defence against *P. aphanis* at the molecular level remain to be clarified. Transcriptome analysis has shown differentially expressed genes (DEGs) related to secondary metabolism, signal transduction, and disease resistance were significantly upregulated and played crucial roles in the early defence response of diploid strawberry against *P. aphanis* [18]. Furthermore, functional identification of candidate genes from the diploid strawberry has enabled the investigation of resistance to *P. aphanis*. These include *FvHsfB1a* [19], *FvMLO* [20], and *FvWRKY42* [21]. Antisense expression of *PpMlo1* conferred resistance in the octoploid strawberry to *P. aphanis*, indicating that the Mlo-based resistance mechanism is functional in strawberry [22]. Moreover, ectopic expression of *AtNPR1* in diploid strawberry showed enhanced resistance to *P. aphanis*, suggesting that *NPR1* confers broad-spectrum disease resistance [23]. Overexpression of *AtELP3* and *AtELP4* in diploid strawberry conferred enhanced resistance to *P. aphanis*, suggesting that *ELP* genes may confer resistance against PM [24]. Recent advances in our understanding of resistance against *P. aphanis* have revealed that it is polygenic and quantitatively inherited [25]. Despite these efforts, little research has focused on the molecular resistance mechanisms of the octoploid strawberry. Most studies have focused on applied research, and particularly on pesticides used in practice. The intensive use of fungicides for disease control is hazardous to the environment and human health [26]. Therefore, recent attention has focused on gaining a better understanding of the resistance mechanisms of the octoploid strawberry against *P. aphanis*.

In this study, we first investigated the fluorescence parameters and the germination percentage of conidia to determine infection time. Next, we analysed the transcriptome of infected leaf tissues during different infection stages in two groups (with and without SA treatment) under greenhouse conditions. Kyoto Encyclopedia of Genes and Genomes (KEGG) enrichment showed that DEGs were mainly involved in phenylpropanoid and flavonoid biosynthesis, hormone signalling transduction, and plant–pathogen

interactions. Moreover, we also detected dynamic patterns of total phenolic compounds, as well as proanthocyanidin (PA) and SA content. Furthermore, we analysed the phylogenetic tree and used RT-qPCR to identify highly homologous proteins, which were used to analyse the correlation between these key genes at the molecular level based on the *Arabidopsis thaliana* model. Our results provide insight into the molecular basis underlying the defence mechanism of the octoploid strawberry response to *P. aphanis*. SA, PAs, total flavonoid content (TFC), and signalling molecules are also potential regulatory compounds involved in SA-induced resistance to *P. aphanis*. This study is the first to characterise the resistance mechanisms of the octoploid strawberry using transcriptome analysis.

Results

Leaf dynamics in response to P. aphanis

To elucidate the mechanisms of the leaf response to *P. aphanis* in strawberry, the cultivar sensitive to *P. aphanis* (Benihoppe) was divided into two groups; one was pre-treated with water (SA⁻) and the other pre-treated with SA (SA⁺). Changes in fluorescence parameters and morphology were determined in a greenhouse environment following inoculation with *P. aphanis*. The maximum and minimum variables in the greenhouse were: 27/7, 28/10, 27/10, 28/9, 28/9, 30/9, 24/9, and 27/9 °C for temperature and 95/47, 95/40, 95/39, 95/58, 95/54, 94/36, 93/54, and 91/49 % for relative humidity throughout the experiment (Fig. 1A). To investigate leaf resistance in response to *P. aphanis*, the conidial germination percentage of *P. aphanis* was recorded over the entire experimental period (Table 1). Visual symptoms (white mycelium) began appearing on leaves at 3 days post-inoculation (dpi) in both the SA⁻ and SA⁺ groups, and obvious differences were observed between the two groups (e.g., there was a larger disease area in SA⁻ leaves than SA⁺). Whereas extensive colonization occurred along the leaf in the SA⁻ group at 7 dpi, only small, restricted colonization was observed in the SA⁺ group (Fig. 1C). The developmental stages of *P. aphanis* were also observed using a microscope (Fig. 1D).

To further ascertain the optimum sampling time, chlorophyll fluorescence parameters in the SA⁻ and SA⁺ groups infected with *P. aphanis* were detected (Fig. 1B). Both groups showed decrease in the F_v/F_m ratio at 1 dpi and an increase at 3 dpi, followed by a continuous decline in F_v/F_m values from 3 to 7dpi. The F_v/F_m ratios in the SA⁺ group were significantly higher than those in the SA⁻ group from 1 to 7 dpi, and coincided with visual symptoms at the corresponding time points (Fig. 1C). Φ_{PSII} showed a continuous decline over the course of the experiment; Φ_{PSII} was significantly higher in the SA⁺ group compared to SA⁻ group from 3 to 7 dpi. The Φ_{NPQ} significantly higher in the SA⁺ group compared to the SA⁻ group from 3 dpi to 7 dpi. In contrast to F_v/F_m , Φ_{PSII} , and Φ_{NPQ} , Φ_{NO} in the SA⁻ group was significantly higher than that in the SA⁺ group from 5 to 7 dpi. In Benihoppe infected with *P. aphanis*, reductions in F_v/F_m , Φ_{PSII} , and Φ_{NPQ} were detected at 3 days prior to the appearance of any visible symptoms. Therefore, these divergent phenotypes (3 dpi) were used in the transcriptome analyses.

Changes in the transcriptome in strawberry leaves infected with P. aphanis

To determine the transcriptome profile of strawberry in response to *P. aphanis*, RNA sequencing (RNA-Seq) analyses were performed on 12 samples of SA⁻ and SA⁺ leaves at 0 and 3 dpi. Approximately 600 million raw reads were obtained in total, and 94, 94, 94, and 92% of the clean reads were mapped to the *F. ananassa_Camarosa* genome (Table S1). FPKM values of DEGs were used to calculate the fold changes of 3DPI⁻/Control⁻ and 3DPI⁺/Control⁺. Principle component analysis (PCA) showed that PC1 and PC2 could explain 64.40% of the total transcript expression level variance, which explained 50.96% of the total detected variation, while the biological replicates contributed another 13.44% of the variability (Fig. S1). Among the two groups, 48,020 transcripts and 45,896 transcript genes were expressed in the strawberry leaves from 3DPI⁻/Control⁻ and 3DPI⁺/Control⁺ leaves, 43,103 genes were commonly expressed in 3DPI⁻/Control⁻ leaves, 2770 genes were expressed only in Control⁻ leaves, and 2147 genes were expressed only in 3DPI⁻ leaves. While 3DPI⁺/Control⁺ had 41,939 commonly expressed genes, 1755 genes were expressed only in Control⁺ and 2202 in 3DPI⁺ leaves. Based on $p\text{-adjust} < 0.05$ and $|\log_2FC| \geq 1$, a total of 4417 and 3754 DEGs were detected in 3DPI⁻/Control⁻ and 3DPI⁺/Control⁺ leaves, respectively. As indicated in Figure S2AB, 2224 genes were upregulated in 3DPI⁺/Control⁺ leaves compared to 2110 in 3DPI⁻/Control⁻. By contrast, a greater number of genes were downregulated genes in 3DPI⁻/Control⁻ (2088) compared to 3DPI⁺/Control⁺ leaves (1530). However, there were commonly 921 genes expressed at two time-points. A great number of DEGs (upregulated of 1476 genes in SA⁻, unregulated of 1565 genes in SA⁺, downregulated of 1801 genes in SA⁻, downregulated of 1268 genes in SA⁺) were noticeable in both groups, indicating that DEGs in response to *P. aphanis* varied greatly.

Based on BIRCH clustering (Fig. S2E), 4417 DEGs were moderately regulated in the SA⁻ group and further divided into 10 clusters: cluster1, cluster4, and cluster6 were upregulated at 3 dpi; cluster2, cluster3, and cluster5 were downregulated at 3 dpi. A total of 3754 DEGs showed pronounced upregulation in the SA⁺ groups and were also obtained 10 sub-clusters: cluster1, cluster2, cluster4, and cluster6 were upregulated at 3 dpi; cluster3 and cluster5 showed a slight downregulation at 3 dpi. Cluster7, cluster8, cluster9, and cluster10 showed irregular changes in both groups. Overall, the results demonstrated that DEGs in the SA⁻ group were delayed compared with the SA⁺ group. Twenty significantly enriched Gene Ontology (GO) terms were mainly categorised as biological process and molecular function (Fig. S3AB). In the SA⁻ group, most genes were involved in oxidation-reduction process, metal ion binding, cation binding, and oxidoreductase activity. By contrast, only single-organism metabolic process, oxidation-reduction process, and oxidoreductase activity were associated with the SA⁺ group. KEGG enrichment analysis (Fig. S3CD) showed some of the same pathways, such as phenylpropanoid biosynthesis, phenylalanine metabolism, and flavonoid biosynthesis. Pathways unique to the SA⁺ group included plant hormone signal transduction and plant-pathogen interactions. We concluded that the genes for phenylpropanoid and flavonoid biosynthesis, hormone signal transduction, and TFs involved in plant-pathogen interaction were important in strawberry and associated with resistance to *P. aphanis*. A large number of DEGs involved in the responses to *P. aphanis* belonged to cluster1, cluster2 and cluster 4.

The flavonoid biosynthesis pathway participates in resistance against P. aphanis

To determine whether exogenous SA could trigger PA accumulation under PM attack, TFC and PA metabolites in the SA+ group were measured (Fig. 2A-C). The SA concentration in the SA+ group at 0 dpi was significantly higher than that in the SA- group and peaked at 3 dpi in both groups (Fig. 2Aa). Moreover, TFC in the SA+ group was higher than that in the SA- group; at 3 dpi, the values were significantly lower in the SA+ group than in the SA- group (Fig. 2Ab). Additionally, PA levels were significantly higher in the SA+ group than in the SA- group (Fig. 2Ac); a similar trend was observed at 3 dpi. Interestingly, TFC and PA were higher in the SA+ group throughout the infection period. To further clarify the regulatory mechanism of SA-triggered PA in strawberry, the regulation of DEGs associated with phenylpropanoid and flavonoid pathways was investigated (Fig. 2C). RNA-Seq showed the upregulated expression of key genes involved in the flavonoid pathway. Transcript levels of 4-coumarate-CoA ligase 2 (4CL), chalcone synthase (CHS), chalcone isomerase (CHI), flavanone 3-hydroxylase (F3H), dihydroflavonol reductase (DFR), leucoanthocyanidin reductase (LAR), anthocyanidin synthase (ANS), and anthocyanidin reductase (ANR) were significantly increased at 3 dpi compared with the control in both groups. Moreover, the expression levels of these genes were also higher in the SA+ group than that in the SA- group (Table S4). Compared with increased expression of UDP-glucose: anthocyanidin: flavonoid glucosyltransferase (UFGT) at the 3DPI- group, expression of UFGT in the 3DPI+ group was markedly downregulated, indicating that SA pretreatment suppressed UFGT to accumulate more PAs. Overall, we suggest a potential role of PAs in enhancing resistance against *P. aphanis*. Consistent with the transcriptomics data, TFC and PA levels were observed in the SA+ group compared with the SA- group. Therefore, we propose that TFC and PAs are potentially important antifungal compounds.

SA biosynthesis occurs in two distinct pathways; the phenylalanine pathway and the ICS1 pathway, from which nearly 95% of SA is produced [27]. The ICS1 pathway involves two steps: the conversion of chorismate to isochorismate, which is first catalyzed by ICS1, followed by the conversion of isochorismate to SA by an unknown enzyme [28]. In this study, two genes encoding ICS1 were downregulated in both groups (Fig. 2C), indicating that exogenous SA did not significantly induce increased production of SA in strawberry. In addition, endogenous SA may be mainly derived from exogenously sprayed SA (Fig. 2Aa).

The salicylic acid signalling pathway contributes to enhanced resistance

GO and KEGG enrichment demonstrated that all DEGs, including *FLS2*, *RPM1*, *CNGC*, *RBOHD*, *CML*, *MEKK*, *NPR*, *TGA*, *JAZ*, *DELLA*, and *PR1*, in the SA- and SA+ groups were related to signal transduction and plant-pathogen interactions (Fig. S4 and Table S5). To identify a possible role for these identified DEGs in the regulation of defence responses, a phylogenetic tree was constructed to show similar topologies with higher bootstrap values (Fig. 3). Heatmap analysis of expression was also performed to investigate expression patterns between the two groups (Fig. 3).

FaFLS2 (*FxaC_10g00870* and *FxaC_9g48710*) and *FaRPM1* (*FxaC_9g38170*) were significantly downregulated in the SA+ group compared to the SA- group, while expression of both genes was always consistently higher in the SA+ group than in SA- group, indicating SA significantly induced the

expression of these resistance genes. Three *FaRPM1* genes (*FxaC_17g37350*, *FxaC_17g37380*, and *FxaC_18g20390*) were significantly downregulated in the SA⁻ group, suggesting they may prevent activation of plant defences against *P. aphanis*. However, others genes were upregulated in the SA⁺ group compared to SA⁻ group, such as *FaRPM1* (*FxaC_23g09840*) and *FaCNGC1* (*FxaC_17g23960*).

Two *FaMEKK* genes (*FxaC_10g49480* and *FxaC_4g34020*) were significantly downregulated in the SA⁺ group compared with no change in the SA⁻ group, whereas *FxaC_16g16370* was also upregulated in both groups. Interestingly, three *FaNPR1* genes (*FxaC_10g12880*, *FxaC_11g10120*, and *FxaC_12g38540*) were markedly downregulated in the SA⁺ group compared with no change in the SA⁻ group. The expression of DEGs from the calmodulin-like (CML) family appeared to be more sharply regulated in the SA⁻ compared with the SA⁺ group. Phylogenetic tree analysis showed clustering of DEGs to *BpBETVIII*, *AtCML44*, *AtCML45*, *AtCML47*, *AtCML-CP1*, *AtCML21*, *AtCML8*, *AtCML27*, *AtCML41*, and *OsCML19*, including *FxaC_23g34420*, *FxaC_5g07320*, *FxaC_23g50900*, *FxaC_24g57620*, *FxaC_17g19620*, *FxaC_18g30960*, *FxaC_14g18440*, *FxaC_12g04650*, *FxaC_9g06650*, *FxaC_16g01580*, *FxaC_2g41240*, *FxaC_1g15840*, and *FxaC_19g08350*. However, expression of all the downregulated DEGs in the Control⁺ group was significantly higher than that in the Control⁻ group (Table S3).

Several key differentially expressed TFs were also identified, such as *TGA*, *JAZ*, *DELLA*, and *WRKY33*. Phylogenetic tree analysis revealed how *FxaC_3g25760* clustered closely to *AtTGA1* and *AtTGA4* (Fig.3). Compared with no change in the SA⁺ group, *FxaC_3g25760* was significantly upregulated in the SA⁻ group, indicating that *FaTGA* negatively regulated SA signalling. Importantly, *FxaC_2g07700* (DELLA protein GAI-like) was significantly downregulated in the SA⁻ group and upregulated in the SA⁺ group (Table. S3). *FaWRKY33* (*FxaC_12g06490*) was substantially downregulated in the SA⁺ group but slightly upregulated in the SA⁻. Moreover, two *FaJAZ* genes (*FxaC_3g09270* and *FxaC_4g31320*) were significantly downregulated in the SA⁻ group but only slightly downregulated in the SA⁺ group. Additionally, *FxaC_20g24100* and *FxaC_20g24200* clustered closely to *AtMYC2*, and were significantly downregulated in the SA⁺ group compared with no change in the SA⁻. The expression of *FxaC_5g41190* and *FxaC_7g01680* (PR1), which clustered to *AtPR1*, was unchanged in the SA⁺ group. Of the five *FaPR1*, *FxaC_7g01820* was significantly upregulated in the SA⁺ group but only slightly upregulated in the SA⁻ group.

The expression pattern of pathogen-related resistance genes

There was a significant increase in the expression of anti-fungal genes from 0 to 3 dpi in the SA⁺ group at the early defence stage. Target genes encoding antifungal compounds (PR1, PR2, PR3, PR5, PR9, and PR10; Fig. 4) in the SA⁻ and SA⁺ groups were measured at each time point. The DEGs revealed similar expression patterns to those measured by RNA-Seq, with significant overexpression in the SA⁺ group, with the exception of PR10, whose expression was significantly downregulated at 0 hpi and slightly upregulated (although not significantly) at 1dpi. However, PR10 was expressed at a significantly higher level from 3 to 7 dpi.

To investigate the defence response involved in SA-induced resistance, the major transcriptional changes (log₂ fold change > 3) in response to *P. aphanis* infection between the 3DAI+ and Control+ groups were monitored (Table. S6), including expression of *PR1* (*FxaC_7g01820*), *PR2* (endo-1,3-glucanase, *FxaC_9g22040* and *FxaC_21g36890*), *PR3* (chitinase, *FxaC_3g11800*), *PR5* (thaumatin-like protein, *FxaC_21g46690* and *FxaC_24g22200*), *PR9* (plant peroxidase, *FxaC_12g01950*), and *PR10* (*FxaC_14g19400*). Expression patterns of the *PR* genes in both groups were further examined by RT-qPCR (Fig. 4). Following SA treatment, the expression of these nine *PR* genes in strawberry leaves between the 3DPI+ and Control+ groups showed a similar trend as that observed with RNA-Seq. SA had a direct influence on *FaPR1*, *FaPR2*, *FaPR3*, *FaPR5*, and *PR10*, as evidenced by the significant difference in expression in the Control+ group compared with the Control-. Moreover, during the test period, the expression of all nine *PR* genes continued for ~5 days. In response to *P. aphanis*, the SA+ group exhibited significantly higher *FaPR1*, *FaPR2-1*, *FaPR2-2*, *FaPR3*, and *FaPR5-1* expression than the SA- group at all experimental time points. Interestingly, at 0 dpi, there was significantly suppression of *FaPR10* expression in the SA+ group.

Genes associated with the SA signalling pathway

To evaluate the phylogenetic relationships of the gene families of strawberry and *Arabidopsis*, protein sequences from different gene families were used to construct an unrooted phylogenetic tree (Fig. S5 and Table. S7). Phylogenetic relationships of the gene families and transcriptomics analyses showed several DEGs related to TFs, as well as SA and JA signalling pathways, such as *NHL3* (*FxaC_17g56190*), *PAD4* (*FxaC_2g34100*), *EDS1* (*FxaC_17g21160*), *WRKY70* (*FxaC_21g59090*), *JUB1* (*FxaC_25g01870*), *AOS1* (*FxaC_6g45880*), *LOX2* (*FxaC_13g21330*), and *JAR1* (*FxaC_26g21700* and *FxaC_28g20590*).

The expression level of *FaNHL* (*FxaC_17g56190*) were 7.95-fold higher in the SA+ group, peaking at 1 dpi in comparison to the SA- group in which *FaNHL* expression was only 3.54-fold higher at the same time point (Fig. 5). The expression of *FaPAD4* in the SA+ group was similar to that of the SA- group. Interestingly, expression of *FaLOX2* in the SA+ group was significantly higher than in the SA- group from 0 to 1 dpi; however, from 3 to 7 dpi the opposite pattern was true, with the SA+ group showing lower expression levels, increasing 1.31-fold at 3 dpi and decreasing again at 7 dpi to ~1.26-fold. Lipase-like *PAD4* (*FaPAD4*, *FxaC_2g34100*), which contributes to plant innate immunity against biotrophic pathogens, was significantly overexpressed in the SA+ group compared with the SA- group throughout the experiment, especially at 3 dpi in the SA+ group (15.01-fold higher than the Control- group) compared with the SA- (6.06-fold higher than the Control- group). Another SA-synthesis gene, enhanced disease susceptibility 1 (*EDS1*, *FxaC_17g21160*), was expressed at a higher level in the SA+ group throughout the experiment period compared with SA- group (Fig. 5). *WRKY70* was differentially expressed in the 3DPI-/Control- group, whereas its expression in the SA+ group was significantly higher than in the SA- group (Fig. 5). Expression of *FaAOS* and *FaJAR1* showed similar patterns across all time points, as they were significantly upregulated at 1 dpi in the SA+ group, whereas there were no significant differences between the SA- and SA+ groups (Fig. 5). Interestingly, the expression of *FaLOX2* in the SA+ group

gradually decreased, being higher than SA- from 0 to 1 dpi, whereas from 3 to 7dpi, it was higher in the SA- group than in the SA+ group.

Discussion

Although comparative transcriptome data has provided insights into the the strawberry defence against *P. aphanis* generated from two diploid strawberry varieties, the molecular mechanisms in octoploid strawberry are not well understood due to difference in the genetic background of the diploid strawberry varieties and the octoploid strawberry. Therefore, identification of key components involved in defence pathways is essential for the creation of disease-resistant varieties. In this study, we analysed strawberry resistance mechanisms against *P. aphanis* by comparing phenotypic differences in two groups in response to PM.

Distinctive phenotypes of the two strawberry groups

A combination of SA treatment plus *P. aphanis* was used. This stressor induced significant differences in F_v/F_m between the two groups. *P. aphanis* induced a decrease in F_v/F_m in the SA- group compared with the SA+ group, especially at 3 dpi in the SA+ group, at which F_v/F_m returned to normal levels. This is possibly because SA could induce the defence against pathogen stress. Furthermore, in the SA+ group, nonphotochemical quenching (NPQ) was significantly higher compared to the SA- at 5 dpi. Moreover, at 3 dpi, the SA+ group exhibited few symptoms. Thus, it was assumed that the energy dissipated through nonregulated mechanisms and was not harmful to the strawberry. In this study, the optimal infection times of 0 and 3 dpi were used in further RNA-Seq analyses. Of the KEGG pathways identified in two groups, the flavanol biosynthesis pathway was the most enriched, indicating the importance of gene regulation of the flavanol metabolite in octoploid strawberry in response to *P. aphanis*. Previous work has shown that genes related to secondary metabolism, signal transduction, transcription factors and disease resistance play important role in defense against *P. aphanis* [18].

SA biosynthesis genes may contribute to resistance against P. aphanis

In *Arabidopsis*, the primary pathway for SA biosynthesis is the ICS1 pathway [29], which also relies on genes, such as EDS1 and PAD4. This pathway triggers early plant defences and the HR independently of PAD4, after which it recruits PAD4 to potentiate plant defences through the accumulation of SA. In this study, *FaICS1* (*FxaC_19g13570*) was downregulated in the SA- group compared to no change in the SA+ group, indicating that *P. aphanis* may suppress expression of this gene. Moreover, EDS1 and PAD4 act upstream of SA accumulation at the infection site, while expression of the EDS1-PAD4 complex can be increased by exogenous SA [30]. Our study showed that SA could stimulate the expression of *FaEDS1* and *FaPAD4* at 0 dpi, which was confirmed by RNA-Seq and RT-qPCR analyses. SA enhanced signal transduction processes, especially expression of membrane proteins, were observed at the initial stage of *P. aphanis* infection. Furthermore, the SA+ group showed a significantly higher SA content compared with the SA- group (Fig. 2). Higher resistance to *P. aphanis* in Benihoppe was also observed in the SA+ group

(Table 1). These results indicate that Benihoppe is not able to activate the rapid accumulation of SA, which is a positive regulator of the defence against biotrophic pathogens.

Increased TFC and PAs in the SA+ group may restrict P. aphanis development

It was recently reported that flavan was induced in the chemical defence against fungal [31, 32]. In this study, we showed that PA level and TFC increased following treatment with SA (Fig. 2). However, SA does not stimulate the flavonoid biosynthetic pathway. SA increased PA accumulation in *Cistus heterophyllus* [33] and in grapevines [34]. In this case, RNA-Seq data showed significant transcriptional upregulation of key flavonoid pathway genes involved in PA synthesis following SA treatment in strawberry (Fig. 2). In particular, *FaGULTs* were significantly downregulated in the SA+ group under *P. aphanis* stress (Fig. 2), indicating that SA treatment could induce and increase PA accumulation. The MBW complex (MYB–bHLH–WD40) regulates the biosynthesis of PAs via directly activation of the genes involved in the late steps of the flavonoid biosynthetic pathway [35]. However, in this study, no homologous *FaMBW* complexes or *FaMYB* were present in Benihoppe, indicating that there may be functional TFs that regulate PA biosynthesis, which will require further investigation.

Cell trans-membrane proteins are involved in reactive oxygen species (ROS) and signalling transduction in the SA– and SA+ groups

It has been shown that SA acts in association with ROS in signalling cascades, leading to resistance [36]. In *Arabidopsis*, *AtrbohD* encodes a key enzyme for ROS production, contributing to host resistance. Moreover, *rbohD* increases susceptibility to pathogens, suggesting that *AtrbohD* plays an important role in resistance to *E. chrysanthemi* [37]. In this study, two *RBOHD* genes (*FxaC_13g23620* and *FxaC_14g16370*) were identified as DEGs, which were all induced significantly higher in the SA+ group compared with the SA– group at 0 dpi (Table S2), indicating that SA plays a crucial role in the accumulation of *RBOHD* genes involved in resistance to PM. Despite these genes being significantly downregulated at 3 dpi in both groups, their expression in the SA+ group was higher than in the SA– group. These results indicate that Benihoppe (a susceptible cultivar) cannot activate a transcriptional program at the initial stage of *P. aphanis* infection (Fig. 6).

FLS2 (LRR receptor-like serine/threonine-protein kinase) family members function as recognition factors of flagellin; recognition results in increased resistance against pathogens [38]. In this study, two *FaFLS2* genes (*FxaC_10g00870* and *FxaC_9g48710*) homologous to *AtFLS2* were downregulated under *P. aphanis* stress in both groups (and were considered DEGs based on our criteria), but their expression was higher in the SA+ group than in the SA– at 0 dpi, indicating that they might be involved in *P. aphanis* resistance in Benihoppe. Our results suggest that Benihoppe is slow to activate any defence responses against pathogen growth. Furthermore, the effector (AvrPto1 or hopD2) from *P. syringae* interacts with FLS2 to block the downstream signalling of the immune response [39]. In addition to FLS2, plant resistance is also triggered by disease resistance protein (RPM1), which is involved in the HR [40]. In this study, three *RPM1* encoding genes (*FxaC_17g37350*, *FxaC_17g37380*, and *FxaC_18g20390*) in SA– group and two genes (*FxaC_23g09840* and *FxaC_9g38170*) in the SA+ group were identified as DEGs

(Table S2). Interestingly, *FxaC_23g09840* was significantly induced by *P. aphanis* only in the SA+ group but was slightly downregulated in the SA- group. We suggest an essential role for this gene in the plant defence response to *P. aphanis* in the SA+ group (Fig. 6). Further study of its molecular function may help reveal the different mechanisms of resistance in the two groups.

Cyclic nucleotide-gated ion channel 2 (CNGC2) has an important roles in pathogen-induced calcium influx and in regulating cell death programs [41]. Through BLASTP analysis, we identified 19 candidate DEGs encoding CNGC in the *Fragaria × ananassa* genome (Table S3). However, phylogenetic tree analysis showed that only *FxaC_9g38170* was homologous to AtCNGC, and was induced by SA pretreatment, and its expression was comparable in the two groups. This result indicated that *FxaC_9g38170* might play a roles in the defence against *P. aphanis* in Benihoppe, which was further confirmed by the results, indicating that *cngc2* leads to a broad-spectrum disease resistance [42].

NDR1/HIN1-like protein 3 (NHL3) belongs to the NHL family, and is a pathogen responsive protein that plays a vital role in plant defence [43]. A previous study showed that *NHL3*-overexpression conferred resistance to *P. syringae* without increased expression of pathogenesis-related genes [44]. Phylogenetic tree analysis showed that FaNHL3 (*FxaC_17g56190*) identified closely to AtNHL3. Particularly, from 0 to 3 dpi, the expression in the SA+ group was significantly higher than in the SA- group, indicating that expression of *FaNHL3* was mediated by the SA pathway. This result indicates that *FaNHL3* may play a crucial role in the defence against PM. However, these results alone do not suggest a regulatory role for the identified DEGs in the activation of downstream signaling components. Therefore, a protein-protein interaction studies are needed in the future.

TFs involved in hormone signalling in the Benihoppe response to P. aphanis

Emerging evidence has demonstrated SA-JA antagonism in many plants [45–47]. It is known that the SA-mediated pathway elevates resistance to biotrophs and is often associated with an increase in necrotrophs. DELLA proteins are able to influence disease by mediating the balance between SA and JA signalling in *Arabidopsis* [48, 49]. In the present study, although *FaDELLA* (*FxaC_2g07700*) showed significant upregulation in the SA+ group (Fig. 2), it was expressed at lower levels in the SA+ group compared with the SA- group at the same time points (Table S2), indicating that SA can influence DELLA accumulation, resulting in attenuate of JA signalling and therefore promotion of *P. aphanis* resistance. DELLA can induce suppression of SA-responsive defence genes [50]. The TFs is JUNGBRUNNEN1 (JUB1) negatively regulates the defence against *P. syringae* via accumulation of DELLA [51]. Here, *FaJUB1* (*FxaC_25g01870*) was significantly downregulated in SA- group at the early infection stage (Table S7), whereas expression in the SA+ group was higher (Fig. 5), resulting in significant resistance at 3dpi (Table 1).

DELLA interacts with JAZ to inhibit JA-responsive transcription factors, especially MYC2, resulting in the suppression of JA-responsive genes [52]. MYC2 is a direct target for JAZ in the JA signalling pathway [53]. In this study, two *FaMYC2* genes (*FxaC_20g24100* and *FxaC_20g24200*) in the SA+ group were identify as DEGs that were significantly downregulated but were not significantly induced by *P. aphanis* in

the SA⁻ group. This suggests that SA may suppress the expression of *FaMYC2*, resulting in enhanced resistance to *P. aphanis*. JAZ plays a crucial role in repressing JA responses, in which the function of MYC2 is repressed by JAZ [54]. Our results showed two *FaJAZ* genes (*FxaC_3g09270* and *FxaC_4g31320*) were significantly downregulated in the SA⁻ group, indicating that *P. aphanis* may induce elevated levels of JA to release MYC2, leading to increased expression of JA-responsive genes.

NPR1 is a key positive regulator of SA signalling transduction and physically interacts with TGA, which is involved in SA-dependent activation of *PR1*, leading to transcriptional regulation of gene defence systems [9, 55]. In the present study, the expression of three *FaNPR1* genes (*FxaC_10g12880*, *FxaC_11g10120*, and *FxaC_12g38540*) was significantly higher in the SA⁺ group compared with the SA⁻ group (Table S2), resulting in significant SA content in leaves at the early stage of infection (Fig. 2). *FaTGA* (*FxaC_3g25760*) clustered closely to group I (AtTGA1 and AtTGA4), which may be involved in the induction of systemic acquired resistance via its interaction with NPR1. Our study showed that *FaTGA* (*FxaC_3g25760*) was significantly downregulated in the SA⁻ group, indicating that at 3 dpi, *P. aphanis* suppresses the levels of SA to inhibit the accumulation of *PR1*. The WRKY family of genes mediates plant defences against various pathogens [56] and controls multiple plant responses [57]. In particular, WRKY33 plays a vital role in resistance to necrotrophs and regulates the antagonistic relationship between the defence pathways [58]. In *Arabidopsis*, *WRKY33* is a downstream component of the JA signalling pathway, resulting in defence responses to necrotrophs [59]. Interestingly, in our study, *FaWRKY33* (*FxaC_12g06490*) was significantly downregulated in the SA⁺ group, suggesting that *P. aphanis* can induce upregulation of *FaWRKY33* at 3 dpi to increase resistance to necrotrophs, resulting in decreased resistance to biotrophs. Importantly, these *FaWRKY33* genes were also upregulated in Benihoppeby *P. aphanis* in the absence of SA treatment. Our study was consistent with previous studies of pathogen strategies [60], in which *P. aphanis* deploys different molecules to interfere with the SA signalling pathway. WRKY70 is another important molecule involved in the balance between SA- and JA-dependent responses [61]. Moreover, WRKY70 positively regulates SA-mediated signalling by increasing expression of EDS1 in *Arabidopsis* [11]. In our experiment, expression of *FaWRKY70* (*FxaC_21g59170*) was significantly upregulated by *P. aphanis* infection in the SA⁺ group but downregulated in the SA⁻ group, supporting our hypothesis that *P. aphanis* interferes with SA signalling. These results suggest that these highly differentially expressed TFs are involved in broad-spectrum resistance of plants to *P. aphanis*, and especially in key node TFs, such as *FaDELLA*, *FaWRKY33*, and *FaWRKY70* (Fig. 6).

Defence-related proteins contribute to enhanced resistance to P. aphanis

In accordance with the results of the resistance performance assays (Table 1), nine DEGs known to regulate PR proteins identified by transcriptome data (log₂ fold change >3) were found to be linked with increased resistance to *P. aphanis*, including PR1, PR2, PR3, PR5, PR9, and PR10. Interestingly, all of these DEGs were specifically resistant to *P. aphanis* or expressed at higher levels in the SA⁺ group compared with the SA⁻ group (Fig. 4, Tables S4). We suggest that the significantly different expression of these PR genes between the two groups might be due to different resistance modes, resulting in enhanced

resistance to *P. aphanis*. On the other hand, differences in biological processes such as increased TFC and PA levels may contribute to the differences in resistance.

Conclusions

We identified different candidate genes in the octoploid strawberry (Benihoppe) response to *P. aphanis* compared to those identified in the study on PR genes and TFs in the diploid strawberry–*P. aphanis* interaction. Based on our results and the SA–JA crosstalk model in *Arabidopsis* [62], an integrated model of the defence response to *P. aphanis* was proposed (Fig. 6). We suggest the following conclusions: (i) *P. aphanis* breaks through the immune system of Benihoppe at early infection in suitable environments; (ii) *P. aphanis* induces drastic changes in gene expression and metabolite production in strawberry; (iii) SA primes the strawberry with enhanced resistance, which is associated with the activation of early recognition genes via SA signalling, rather than by SA synthesis; (iv) PA accumulation and upregulation of PR genes are observed during the resistance response to *P. aphanis*; and (v) several TFs involved in phytohormone signalling pathway contributes to resistance to *P. aphanis*. Comparative transcriptome analysis enabled us to uncover a novel resistance mechanism associated with SA signalling, followed by significant resistance against *P. aphanis*. From the model presented in Figure 6, these results suggest that SA-induced TFC, PAs, and PR proteins act as direct antifungal compounds, whereas TFs may play an essential regulatory role in strawberry defence against *P. aphanis*, especially in balancing biotrophs and necrotrophs. Further research should be conducted using transgenic plants to identify the targets of these TFs. This study lays the foundation for further exploration of the molecular mechanisms of resistance to *P. aphanis* in strawberry, and provides new strategies for improving strawberry varieties through genetic engineering.

Methods

Plant materials

Seedlings of strawberry (*Fragaria × ananassa* Duch.) cv. Benihoppe were provided by the National Germplasm Repository of Strawberry, Beijing Academy of Agriculture and Forestry Sciences, China. The experimental plants were propagated from runners, which were rooted in 5-cm diameter pots filled with a 1:1:1 mixture of peat: vermiculite: perlite and subsequently transplanted in a greenhouse on September 15, 2018 into 20-cm diameter pots filled with a 1:1:1 mixture of peat: vermiculite: perlite. The inoculation experiment was conducted in a plastic greenhouse at Beijing Forestry University. The growth conditions during the experiment period are shown in Figure 1A. No fungicides were applied, and fertiliser was added according to agricultural practice.

P. aphanis inoculation and SA treatment

P. aphanis inoculation was performed one month later on October 15, 2018. The strawberry (Benihoppe) leaf was infected with *P. aphanis* by gentle tapping from an infected strawberry leaf. All experimental

groups were placed in a greenhouse under the growth conditions described above. Eighty plants were split into two subgroups containing 40 plants each: SA untreated group (SA⁻) and SA treated group (SA⁺). Four hours before inoculation with *P. aphanis*, the SA⁻ group was sprayed with water, and at the same time SA⁺ group was sprayed with exogenous SA (2mM) using an atomizer onto the upper fully leaves until it ran off. Three replicates were sampled for each infection time. Randomly ten upper young leaves from each group were sampled at 0, 1, 3, 5, and 7 dpi and RNA was extracted. Samples were immersed in liquid nitrogen and kept at -80 °C until further analysis. This study evaluated four conditions: water treatment and no inoculation (Control⁻); SA treatment and no inoculation (Control⁺); water treatment with inoculation at 3 dpi (3DPI⁻); and SA treatment with inoculation at 3 dpi (3DPI⁺).

TFC and PAs determination

Total flavonoid content (TFC) was determined by a colorimetric method, according to plant total phenol test kit (A142-1-1, Nanjing Jiancheng Bioengineering Institute, Nanjing, China). Briefly, sodium nitrite was added to sample, and then aluminum chloride was added. Finally, sodium hydroxide was added to the mixture. After 2 hours, the sample extract was centrifuged for 10 min at 10,000 rpm, and the absorbance of the supernatant was read at 502 nm and compared with that of rutin standards. The flavonoid content is expressed as mg/g DW.

Proanthocyanidins content (PAs) was determined according to plant proanthocyanidins test kit (A144-1-1, Nanjing Jiancheng Bioengineering Institute, Nanjing, China). The chromogenic solution, vanillin solution: hydrochloric acid solution = 1:1, ready-to-use. Briefly, methanol was added to sample. After 20 min stirring, the mixture was centrifuged for 20 min at 3000 rpm, and then supernatant was added to the chromogenic solution. The absorbance of the solution was measured at 500 nm and compared with that of rutin standards.

Extraction of endogenous free SA

Phytohormones were analyzed according to the standard protocol described by Pan et al [63]. Triplicate samples of 50 mg of leaves were used, and liquid chromatography-mass spectrometry (Waters Corp., Milford, MA) analyses of SA were performed by the Testing and Analysis Center of Beijing Forestry University, Beijing, China.

Assays of fluorescence parameters

The Imaging-PAM Chlorophyll Fluorometer (Walz, Effeltrich, Germany) was used to determine photosynthetic parameters of infected strawberry leaves [64]. Plantlets were prepared with a 20 min dark treatment. Using the Imaging-PAM, Chlorophyll Fluorometer, dark-treatment fluorescence yield, F_0 , and the maximum fluorescence yield, F_m , were determined. Walz software used the formula $F_v/F_m = (F_m - F_0)/F_m$ to calculate the maximal PSII quantum yield. The current fluorescence yield, F_t and the maximum light-adapted fluorescence, F_m' , in the presence of actinic illumination of $400 \mu\text{mol m}^{-2} \text{s}^{-1}$ were used to compute the effective PSII quantum yield $[Y(II) = (F_m' - F_t)/F_m']$. NPQ was determined as the quotient $(F_m -$

$F_m)/F_m$. The non-regulated energy dissipation of PSII quantum yield Y (NO) was obtained using the following formula: $Y(NO) = 1/(NPQ+1+qL(F_m/F_0.1))$. Following the kinetics recording, Walz software used areas of interest that were randomly selected from corresponding surrounding areas of infected leaves. For each treatment, three plants were used and the values were averaged.

Light microscopy

Light microscopy analyses of the development of *P. aphanis* [65] were performed on leaf discs (20 mm diameter) randomly excised from infected leaves at 0, 1, 3, 5, 7 dpi. Leaf disc were stained by boiling for 2 min in alcoholic lactophenol trypan blue (10 mL ethanol, 10 mL phenol, 10 mL water, 10 mL lactic acid, and 10 mg trypan blue). The stained discs were cleared in chloral hydrate (2.5 g dissolved in 1 mL of water) overnight at room temperature. Cleared leaves were mounted under coverslips in 50% glycerol and observed using a Leica DM2500. *P. aphanis* was examined using confocal laser scanning microscopy (Heidelberg Engineering GmbH, Germany).

Transcriptome analysis

To identify the key pathways in the strawberry–*P. aphanis* interaction, samples were collected from twelve samples and were used for RNA-Seq analysis (Table S1). Total RNA was extracted and an RNA-Seq transcriptome library was prepared using the TruSeq™ RNA Sample Preparation Kit (Illumina, San Diego, CA, USA). Sequence reads were aligned using the sequence assembly of the octoploid strawberry genome annotation *Fragaria_x_ananassa_Camarosa_Genome_v1.0.a1* as a reference, which is available at GDR (<https://www.rosaceae.org/>) and SGR (<http://bioinformatics.towson.edu/strawberry/>). Empirical Analysis of Digital Gene Expression in R (EdgeR) software (<http://www.bioconductor.org/packages/2.12/bioc/html/edgeR.html>) was used for differential expression analyses.

Multiple sequence alignment and phylogenetic analysis

The gene IDs of the genes from the strawberry are shown in Table S3 and S5. The full predicted amino acid sequences of the genes from the two plant species (strawberry and Arabidopsis) were aligned using ClustalW. A Neighbor-Joining (NJ) phylogenetic tree was constructed by MEGA 7.0 software. Bootstrap test were carried out with 1000 replicates for evaluating the statistical reliability of the phylogenetic tree.

Validation of RNA-Seq data by RT–qPCR

Ten transcriptomic genes from the RNA-Seq analysis were selected and validated by RT–qPCR. Primers were designed using Primer Premier 5.0. Total RNA from leaves was isolated from each sample using EASYspin and the plant RNA Mini Kit (Aidlab, Beijing, China). Subsequently, RNase-free DNase was used to treat total RNA (2 µg) to remove genomic DNA. cDNA was synthesized using GoScript Reverse Transcription Kit according to the manufacturer's instructions (CW BIO, Jiangsu, China). RT–qPCR was

performed in 20µl reactions using an Applied Biosystem 7500 real-time PCR system. Gene expression was calculated using the $2^{-\Delta\Delta C_t}$ method and normalised using two *FaACTIN* genes as internal. Reactions were performed with three biological replicates. The Primers used for RT-qPCR are listed in Supplementary Table S8.

Statistical analysis

Differences were analysed using a one-way analysis of variance with Fisher's least significant difference test. P-value ≤ 0.05 were considered statistically significant. All analyses were performed using Origin 8.0 software (OriginLab Corp., <https://www.originlab.com/>).

Abbreviations

DEG: Differentially expressed gene

FPKM: Fragments per kilobase of transcript per million

F_v/F_m : photosynthetic efficiency

GO: Gene ontology

HR: Hypersensitive response

KEGG: Kyoto encyclopedia of genes and genomes

NPQ: Nonphotochemical quenching

PCA: Principal component analysis

PR: Pathogenesis-related

RT-qPCR: Real-time quantitative polymerase chain reaction

RNA-Seq: RNA-sequencing

ROS: Reactive oxygen species

SA: Salicylic acid

TFC: Total flavone content

TFs: Transcription factors

Declarations

Ethics approval and consent to participate

Not applicable.

Consent for publication

Not applicable.

Availability of data and material

All data sustaining the results in this study are included in this article or its supplementary information files. The raw sequence data reported in this paper have been deposited in the Genome Sequence Archive (Genomics, Proteomics & Bioinformatics 2017) in BIG Data Center (Nucleic Acids Res 2018), Beijing Institute of Genomics (BIG), Chinese Academy of Sciences, under accession numbers [PRJCA001734](#), which are publicly accessible at <https://bigd.big.ac.cn/gsa>.

Competing interests

The authors declare no conflicts of interest.

Funding

This work was supported by National Natural Science Foundation of China (Number 31870571).

Authors' contributions

JF conceptualized the work and designed experiments. JF and MZ conducted the expression analyses and analysed the data. JF and KNY wrote the draft manuscript. JF, WTY, and CXZ edited the manuscript. All the authors have read and approved the final manuscript.

Acknowledgements

We gratefully acknowledge Kun Shi, for her help with plant propagation and technical assistance.

Supplementary information

Additional file 1:

Figure S1. Principle component analysis of the RNA sequencing samples. *Figure S2.* DEGs in SA⁻ and SA⁺ strawberry leaves. (A) The number of DEGs up- or downregulated at 3 DPI in both groups. (B) Heatmap generated from the DEGs from RNA-Seq analysis comparing the fold changes in gene expression during the infection stage (3DPI⁻/Control⁻ and 3DPI⁺/Control⁺). Heatmap colours represent gene expression fold-change levels based on the provided colour key scale; red = upregulated expression, blue = downregulated expression, and white = no change in expression. (C) Venn diagrams of the number of DEGs between SA⁻ and SA⁺ groups. (D) Venn diagram showing a cross-comparison of the up- and downregulated genes from both groups. (E) Cluster analysis of DEGs in the SA⁻ and SA⁺ groups based

on the BIRCH method. *Figure S3*. (A, B) Significantly enriched Gene Ontology (GO) biological processes in the 3DPI/Control groups. The y-axis represents significantly enriched GO processes (false discovery rate < 0.05). The x-axis indicates the total number of genes annotated to each GO process. Red and blue sections represent downregulated and upregulated genes, respectively. (C, D) KEGG enrichment pathways (Top 20) for Control- vs. 3DPI- and Control+ vs. 3DPI+ groups. The rich factor indicates the degree of enrichment. The colour and size of the dots indicate the range of the q-value and gene number, respectively. *Figure S4*. Hierarchical clustering heatmap for DEGs in the 3DPI-/Control- and 3DPI+/Control+ groups. (A) Cluster analysis of DEGs involved in plant hormone signalling between the 3DPI- and Control- groups; (B) cluster analysis of DEGs involved in plant hormone signalling between the 3DPI+ and Control+ groups; (C) cluster analysis of DEGs involved in plant-pathogen interactions between the 3DPI- and Control- groups; and (D) cluster analysis of DEGs involved in plant-pathogen interactions between the 3DPI+ and Control+ groups. Differences are highlighted in blue (downregulation) and red (upregulation). *Figure S5*. Phylogenetic tree analysis of key genes in Arabidopsis and octoploid strawberry. Numbers at branches indicate posterior probabilities and bootstrap percentages based on 1000 replicates.

Additional file 2:

Table S1. RNA-Seq Reads and Reads Mapping. *Table S2*. Differentially expressed genes in 3DPI-/Control- ($|\log_2FC| > 1$). *Table S3*. Differentially expressed genes in 3DPI+/Control+ ($|\log_2FC| > 1$). *Table S4*. Significant DEGs involved in flavonoid pathway between 3DPI+/Control+. *Table S5*. Significant DEGs involved in plant hormone transduction pathway and plant-pathogen interaction pathway between 3DPI+/Control+ and 3DPI-/Control-. *Table S6*. Significant DEGs (\log_2 fold change >3) in 3DPI+/Control+. *Table S7*. Significant DEGs-associated with SA signaling pathway between 3DPI+/Control+ and 3DPI-/Control-. *Table S8*. Primer sequences and parameters derived from RT-qPCR analysis.

References

1. Jones, J. D. and J. L. Dangl, *The plant immune system*. nature, 2006. 444(7117): p. 323.
2. Chisholm, S. T., et al., *Host-microbe interactions: shaping the evolution of the plant immune response*. Cell, 2006. 124(4): p. 803–814.
3. Braun, U., et al., *The taxonomy of the powdery mildew fungi*. The powdery mildews: a comprehensive treatise, 2002: p. 13–55.
4. Takamatsu, S., *Molecular phylogeny reveals phenotypic evolution of powdery mildews (Erysiphales, Ascomycota)*. Journal of general plant pathology, 2013. 79(4): p. 218–226.

5. Glawe, D. A., *The powdery mildews: a review of the world's most familiar (yet poorly known) plant pathogens*. Annual review of phytopathology, 2008. 46.
6. Kuhn, H., et al., *Biotrophy at its best: novel findings and unsolved mysteries of the Arabidopsis-powdery mildew pathosystem*. The Arabidopsis Book/American Society of Plant Biologists, 2016. 14.
7. Robert-Seilaniantz, A., M. Grant, and J. D. Jones, *Hormone crosstalk in plant disease and defense: more than just jasmonate-salicylate antagonism*. Annual review of phytopathology, 2011. 49: p. 317–343.
8. Spoel, S. H., et al., *NPR1 modulates cross-talk between salicylate- and jasmonate-dependent defense pathways through a novel function in the cytosol*. The Plant Cell, 2003. 15(3): p. 760–770.
9. Johnson, C., E. Boden, and J. Arias, *Salicylic acid and NPR1 induce the recruitment of trans-activating TGA factors to a defense gene promoter in Arabidopsis*. The Plant Cell, 2003. 15(8): p. 1846–1858.
10. Zander, M., et al., *Repression of the Arabidopsis thaliana jasmonic acid/ethylene-induced defense pathway by TGA-interacting glutaredoxins depends on their C-terminal ALWL motif*. Molecular plant, 2012. 5(4): p. 831–840.
11. Li, J., G. Brader, and E. T. Palva, *The WRKY70 transcription factor: a node of convergence for jasmonate-mediated and salicylate-mediated signals in plant defense*. The Plant Cell, 2004. 16(2): p. 319–331.
12. Spoel, S. H. and X. Dong, *Making sense of hormone crosstalk during plant immune responses*. Cell host & microbe, 2008. 3(6): p. 348–351.
13. Thaler, J. S., P. T. Humphrey, and N. K. Whiteman, *Evolution of jasmonate and salicylate signal crosstalk*. Trends in plant science, 2012. 17(5): p. 260–270.
14. Ainsworth, G. C., *Ainsworth & Bisby's dictionary of the fungi*. 2008: Cabi.
15. Folta, K. M. and S. E. Gardiner, *Genetics and Genomics of Rosaceae*. 2009.
16. Zhang, Y., et al. *The current progress in strawberry breeding in China*. in *VIII International Strawberry Symposium 1156*. 2016.
17. Edger, P. P., et al., *Origin and evolution of the octoploid strawberry genome*. Nature genetics, 2019. 51(3): p. 541.
18. Jambagi, S. and J. M. Dunwell, *Global Transcriptome analysis and identification of differentially expressed genes after infection of Fragaria Vesca with powdery mildew (Podosphaera aphanis)*. Transcriptomics: Open Access, 2015. 3(1).
19. Hu, Y., et al., *Identification, isolation, and expression analysis of heat shock transcription factors in the diploid woodland strawberry Fragaria vesca*. Frontiers in plant science, 2015. 6: p. 736.

20. Jambagi, S. and J. M. Dunwell, *Identification and expression analysis of Fragaria vesca MLO genes involved in interaction with powdery mildew (Podosphaera aphanis)*. Journal of Advances in Plant Biology, 2017. 1(1): p. 40–54.
21. Wei, W., et al., *Ectopic expression of FvWRKY42, a WRKY transcription factor from the diploid woodland strawberry (Fragaria vesca), enhances resistance to powdery mildew, improves osmotic stress resistance, and increases abscisic acid sensitivity in Arabidopsis*. Plant science, 2018. 275: p. 60–74.
22. Jiwan, D., et al., *Antisense expression of peach mildew resistance locus O (PpMlo1) gene confers cross-species resistance to powdery mildew in Fragaria x ananassa*. Transgenic research, 2013. 22(6): p. 1119–1131.
23. Silva, K. J. P., et al., *The Arabidopsis NPR1 gene confers broad-spectrum disease resistance in strawberry*. Transgenic research, 2015. 24(4): p. 693–704.
24. Silva, K. J. P., et al., *The Arabidopsis ELP3/ELO3 and ELP4/ELO1 genes enhance disease resistance in Fragaria vesca L*. BMC plant biology, 2017. 17(1): p. 230.
25. Cockerton, H. M., et al., *Identification of powdery mildew resistance QTL in strawberry (Fragaria x ananassa)*. Theoretical and applied genetics, 2018. 131(9): p. 1995–2007.
26. Pertot, I., et al., *Integrating biocontrol agents in strawberry powdery mildew control strategies in high tunnel growing systems*. Crop protection, 2008. 27(3–5): p. 622–631.
27. Vlot, A. C., D. M. A. Dempsey, and D. F. Klessig, *Salicylic acid, a multifaceted hormone to combat disease*. Annual review of phytopathology, 2009. 47: p. 177–206.
28. Strawn, M. A., et al., *Arabidopsis isochorismate synthase functional in pathogen-induced salicylate biosynthesis exhibits properties consistent with a role in diverse stress responses*. Journal of Biological Chemistry, 2007. 282(8): p. 5919–5933.
29. D'Maris Amick Dempsey, A. C., M. C. W. Vlot, and F. K. Daniel, *Salicylic acid biosynthesis and metabolism*. The Arabidopsis book/American Society of Plant Biologists, 2011. 9.
30. Aviv, D. H., et al., *Runaway cell death, but not basal disease resistance, in lsd1 is SA-and NIM1/NPR1-dependent*. The Plant Journal, 2002. 29(3): p. 381–391.
31. Wang, L., et al., *The transcription factor MYB115 contributes to the regulation of proanthocyanidin biosynthesis and enhances fungal resistance in poplar*. New Phytologist, 2017. 215(1): p. 351–367.
32. Ullah, C., et al., *Salicylic acid activates poplar defense against the biotrophic rust fungus Melampsora larici-populina via increased biosynthesis of catechin and proanthocyanidins*. New Phytologist, 2019. 221(2): p. 960–975.

33. López-Orenes, A., et al., *Changes in phenolic metabolism in salicylic acid-treated shoots of Cistus heterophyllus*. Plant Cell, Tissue and Organ Culture (PCTOC), 2013. 113(3): p. 417–427.
34. Wang, H., et al., *Effect of salicylic acid on the gene transcript and protein accumulation of flavonoid biosynthesis-related enzymes in Vitis vinifera cell suspension cultures*. HortScience, 2017. 52(12): p. 1772–1779.
35. Hichri, I., et al., *Recent advances in the transcriptional regulation of the flavonoid biosynthetic pathway*. Journal of experimental botany, 2011. 62(8): p. 2465–2483.
36. Torres, M. A., J. D. Jones, and J. L. Dangl, *Reactive oxygen species signaling in response to pathogens*. Plant physiology, 2006. 141(2): p. 373–378.
37. Fagard, M., et al., *Arabidopsis thaliana expresses multiple lines of defense to counterattack Erwinia chrysanthemi*. Molecular plant-microbe interactions, 2007. 20(7): p. 794–805.
38. Gómez-Gómez, L., Z. Bauer, and T. Boller, *Both the extracellular leucine-rich repeat domain and the kinase activity of FLS2 are required for flagellin binding and signaling in Arabidopsis*. The Plant Cell, 2001. 13(5): p. 1155–1163.
39. Nguyen, H. P., et al., *Two virulence determinants of type III effector AvrPto are functionally conserved in diverse Pseudomonas syringae pathovars*. New phytologist, 2010. 187(4): p. 969–982.
40. Grant, M. R., et al., *Structure of the Arabidopsis RPM1 gene enabling dual specificity disease resistance*. Science, 1995. 269(5225): p. 843–846.
41. Köhler, C., et al., *Developmentally regulated expression of a cyclic nucleotide-gated ion channel from Arabidopsis indicates its involvement in programmed cell death*. Planta, 2001. 213(3): p. 327–332.
42. Clough, S. J., et al., *The Arabidopsis dnd1 “defense, no death” gene encodes a mutated cyclic nucleotide-gated ion channel*. Proceedings of the National Academy of Sciences, 2000. 97(16): p. 9323–9328.
43. Varet, A., et al., *NHL25 and NHL3, two NDR1/HIN1-like genes in Arabidopsis thaliana with potential role(s) in plant defense*. Molecular plant-microbe interactions, 2002. 15(6): p. 608–616.
44. Varet, A., et al., *The Arabidopsis NHL3 gene encodes a plasma membrane protein and its overexpression correlates with increased resistance to Pseudomonas syringae pv. tomato DC3000*. Plant physiology, 2003. 132(4): p. 2023–2033.
45. Takahashi, H., et al., *Antagonistic interactions between the SA and JA signaling pathways in Arabidopsis modulate expression of defense genes and gene-for-gene resistance to cucumber mosaic virus*. Plant and cell physiology, 2004. 45(6): p. 803–809.

46. Wei, J., et al., *Reciprocal crosstalk between jasmonate and salicylate defence-signalling pathways modulates plant volatile emission and herbivore host-selection behaviour*. *Journal of experimental botany*, 2014. 65(12): p. 3289–3298.
47. Ding, L.-N., et al., *Investigating interactions of salicylic acid and jasmonic acid signaling pathways in monocots wheat*. *Physiological and Molecular Plant Pathology*, 2016. 93: p. 67–74.
48. Hou, X., et al., *DELLAs modulate jasmonate signaling via competitive binding to JAZs*. *Developmental cell*, 2010. 19(6): p. 884–894.
49. Yang, D.-L., et al., *Plant hormone jasmonate prioritizes defense over growth by interfering with gibberellin signaling cascade*. *Proceedings of the National Academy of Sciences*, 2012. 109(19): p. E1192-E1200.
50. Achard, P., et al., *Plant DELLAs restrain growth and promote survival of adversity by reducing the levels of reactive oxygen species*. *Current Biology*, 2008. 18(9): p. 656–660.
51. Shahnejat-Bushehri, S., et al., *JUB1 suppresses Pseudomonas syringae-induced defense responses through accumulation of DELLA proteins*. *Plant signaling & behavior*, 2016. 11(6): p. e1181245.
52. Hong, G. J., et al., *Arabidopsis MYC2 interacts with DELLA proteins in regulating sesquiterpene synthase gene expression*. *Plant Cell*, 2012. 24(6): p. 2635–2648.
53. Zhai, Q., et al., *Phosphorylation-coupled proteolysis of the transcription factor MYC2 is important for jasmonate-signaled plant immunity*. *PLoS genetics*, 2013. 9(4): p. e1003422.
54. Melotto, M., et al., *A critical role of two positively charged amino acids in the Jas motif of Arabidopsis JAZ proteins in mediating coronatine-and jasmonoyl isoleucine-dependent interactions with the COI1 F-box protein*. *The Plant Journal*, 2008. 55(6): p. 979–988.
55. Despres and C., *The Arabidopsis NPR1 Disease Resistance Protein Is a Novel Cofactor That Confers Redox Regulation of DNA Binding Activity to the Basic Domain/Leucine Zipper Transcription Factor TGA1*. *Plant Cell*, 2003. 15(9): p. 2181–91.
56. Pandey, S. P. and I. E. Somssich, *The role of WRKY transcription factors in plant immunity*. *Plant physiology*, 2009. 150(4): p. 1648–1655.
57. Rushton, P. J., et al., *WRKY transcription factors*. *Trends in plant science*, 2010. 15(5): p. 247–258.
58. Zheng, Z., et al., *Arabidopsis WRKY33 transcription factor is required for resistance to necrotrophic fungal pathogens*. *The Plant Journal*, 2006. 48(4): p. 592–605.
59. Birkenbihl, R. P., C. Diezel, and I. E. Somssich, *Arabidopsis WRKY33 Is a Key Transcriptional Regulator of Hormonal and Metabolic Responses toward Botrytis cinerea Infection*. *Plant Physiology*, 2012. 159(1):

p. 266–285.

60.Qi, G., et al., *Pandemonium breaks out: Disruption of salicylic acid-mediated defense by plant pathogens*. Molecular plant, 2018.

61.Li, J., et al., *WRKY70 modulates the selection of signaling pathways in plant defense*. The Plant Journal, 2006. 46(3): p. 477–491.

62.Spoel, S. H. and X. Dong, *How do plants achieve immunity? Defence without specialized immune cells*. Nature reviews immunology, 2012. 12(2): p. 89.

63.Pan, X., R. Welti, and X. Wang, *Quantitative analysis of major plant hormones in crude plant extracts by high-performance liquid chromatography–mass spectrometry*. Nature protocols, 2010. 5(6): p. 986.

64.Behr, M., et al., *The hemibiotroph Colletotrichum graminicola locally induces photosynthetically active green islands but globally accelerates senescence on aging maize leaves*. Molecular plant-microbe interactions, 2010. 23(7): p. 879–892.

65.Inada, N. and E. A. Savory, *Inhibition of prepenetration processes of the powdery mildew Golovinomyces orontii on host inflorescence stems is reduced in the Arabidopsis cuticular mutant cer3 but not in cer1*. Journal of general plant pathology, 2011. 77(5): p. 273.

Table 1

TABLE 1. Percentage of *P. aphanis* conidial germination on untreated and SA-treated strawberry leaves.

DPI	1	3	5	7
UC (SA-)	58.46 ± 6.47 ^a	46.45 ± 8.35 ^a	40.22 ± 5.94 ^a	36.64 ± 6.64 ^a
UC (SA+)	78.36 ± 4.82 ^b	62.35 ± 7.95 ^b	56.85 ± 6.10 ^b	46.62 ± 4.23 ^b
GC (SA-)	41.54 ± 8.31 ^a	46.19 ± 5.97 ^a	32.33 ± 3.64 ^a	27.87 ± 4.25 ^a
GC (SA+)	21.64 ± 4.63 ^b	35.31 ± 7.69 ^b	30.82 ± 5.21 ^a	34.67 ± 6.36 ^b
CO (SA-)	0	7.36 ± 1.55 ^a	27.45 ± 4.77 ^a	35.49 ± 4.66 ^a
CO (SA+)	0	2.34 ± 0.83 ^b	12.33 ± 2.53 ^b	18.71 ± 2.84 ^b

UC, ungerminated conidia; GC, germinated conidia without forming appresoria; CO, germinated conidia with conidiophore. Data are means of five replicates ± standard deviation. Different letters at each time point represent significant differences among treatments at $P < 0.05$. DPI: days post-inoculation.

Figures

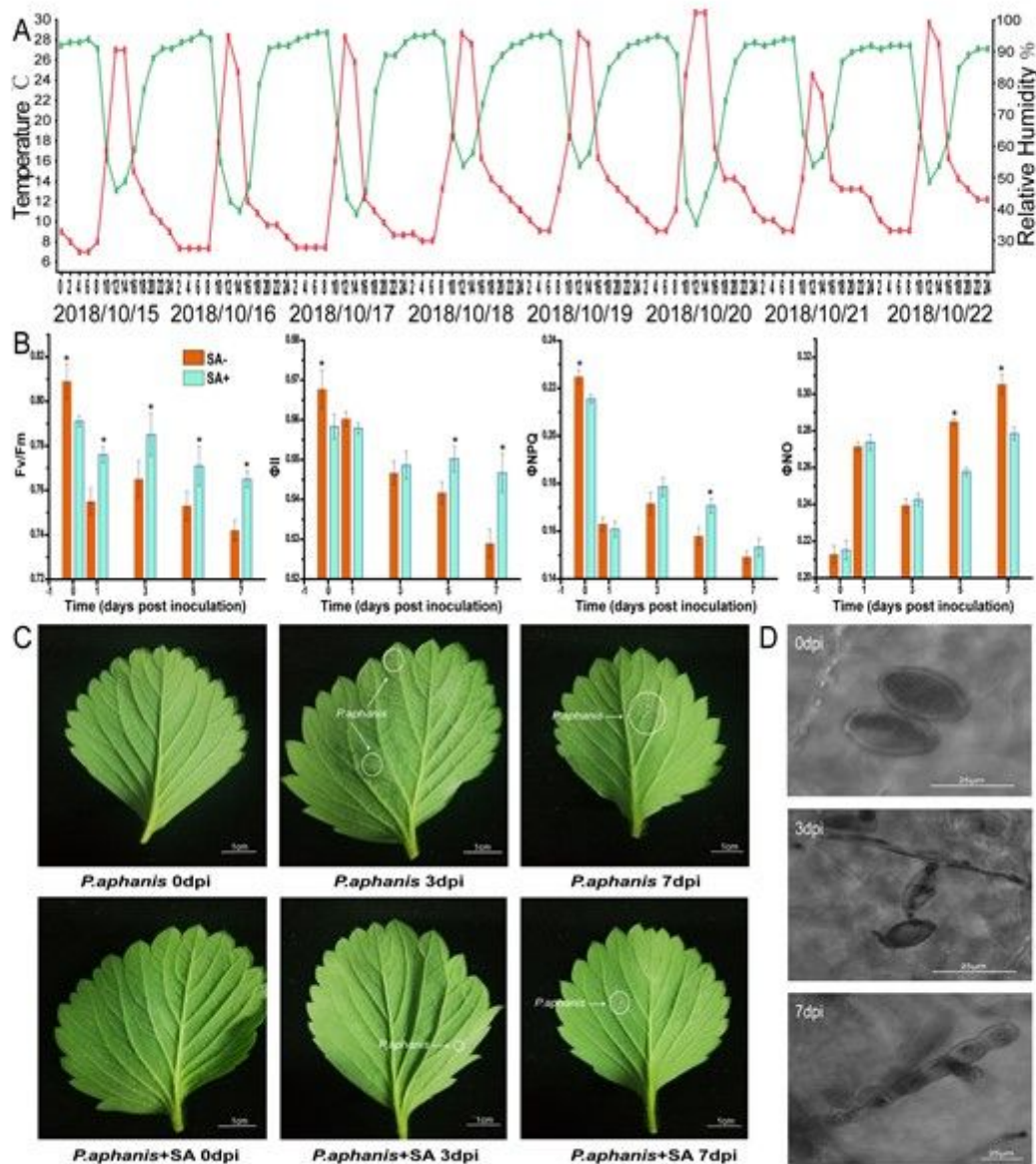


Figure 1

(A) Temperature and humidity in the greenhouse during the experimental period. The data were collected every 2 h from October 15 to October 22, 2018. (B) Time course of strawberry leaf (Benihoppe) responses to infection with *P. aphanis*. Changes in the chlorophyll fluorescence parameters Fv/Fm, Φ_{II} , Φ_{NPQ} , and Φ_{NO} were measured in leaves inoculated with *P. aphanis*. Measurements were taken at 0, 1, 3, 5, and 7 days post-inoculation (DPI). Fv/Fm was determined for 20 min dark-adapted leaves following initial exposure of plants to a saturating light pulse. All values are expressed as mean \pm standard error; N = 3 for Fv/Fm, Φ_{II} , Φ_{NPQ} , and Φ_{NO} measurements. (C) Photographic documentation of the progression of *P. aphanis* infection in strawberry (Benihoppe) leaves treated with SA (SA+) or untreated (SA-) at different time points after inoculation (0, 3, and 7 DPI). Bar = 1 cm. (D) *P. aphanis* conidial germination on strawberry leaves at different time points.

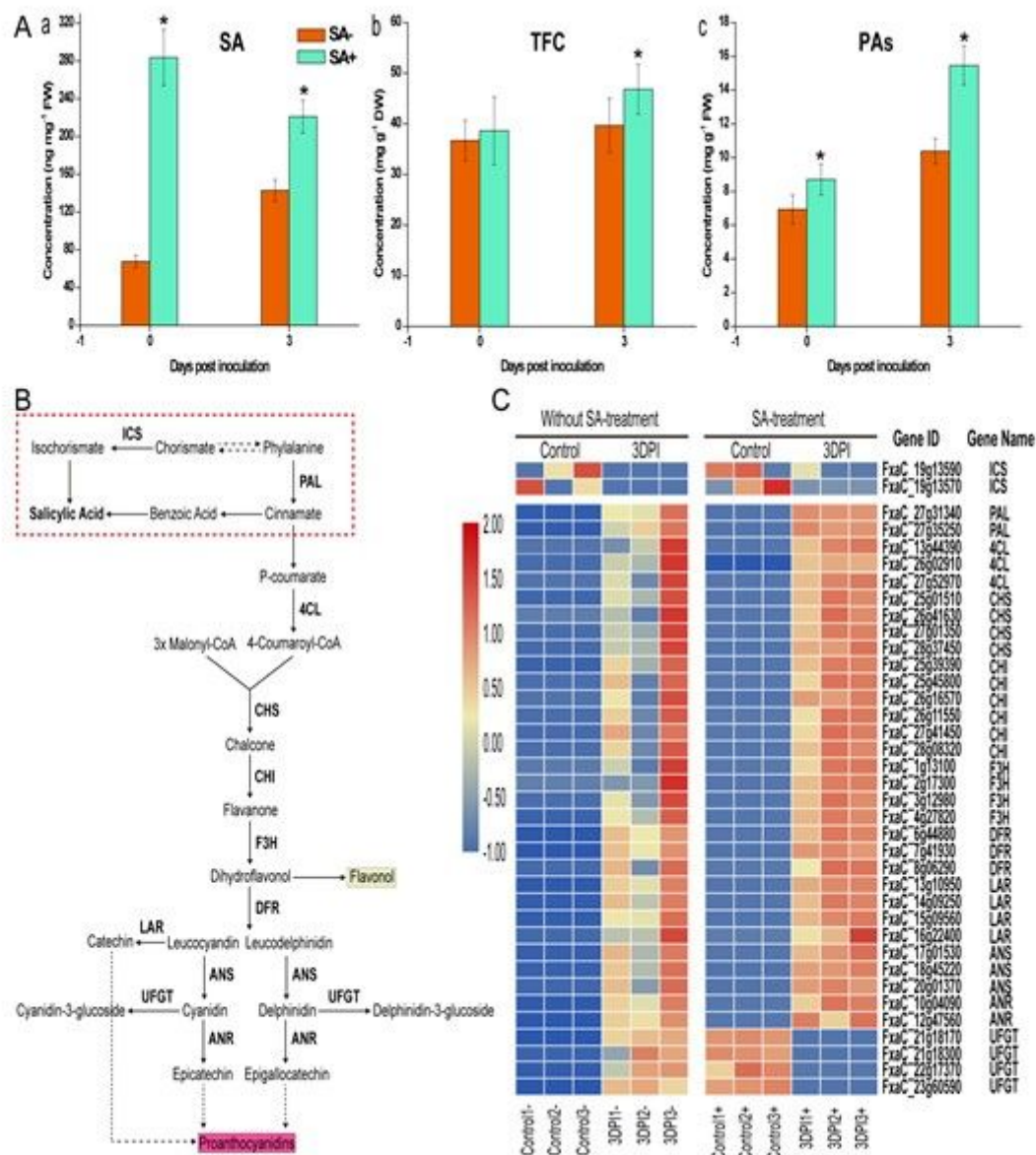


Figure 2

Salicylic acid (SA) content, total flavonoid content (TFC), and proanthocyanidins (PAs) in *P. aphani*-infected strawberry leaves in the SA+ and SA- groups. (A) Concentration of SA, TFC, and PAs in strawberry leaves with or without SA treatment at two different time points. Data are expressed as the mean \pm standard deviation (SD) of three biological replicates. Different letters above the bar indicate statistically significant differences between groups at the same time point ($P < 0.05$). (B) Flavonoid pathway results in the formation of PAs. (C) Relative expression of PA biosynthesis genes. Heatmap was generated using the average values [$\log_{10}(\text{FPKM}+1)$] of three biological samples per treatment.

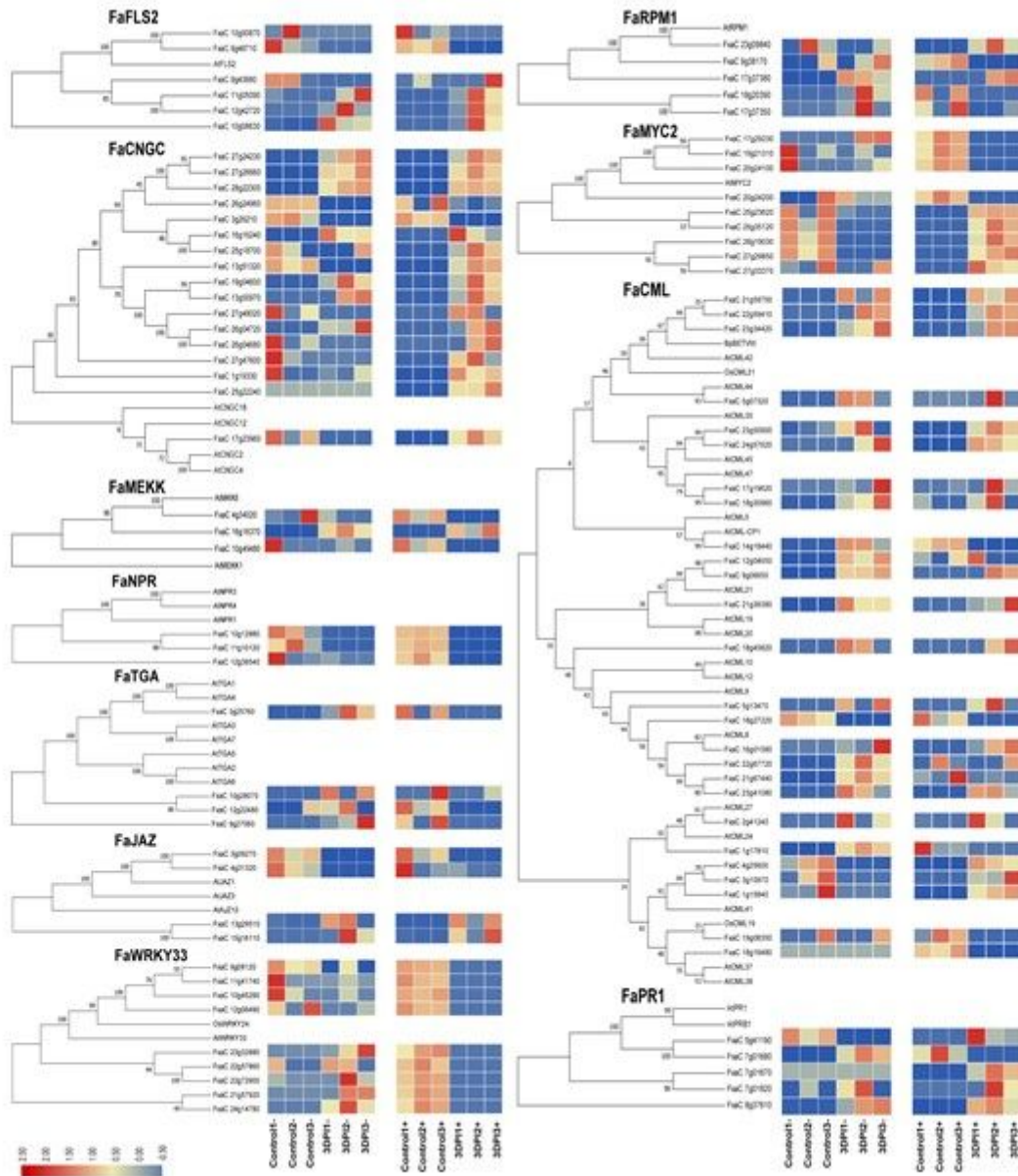


Figure 3

Differentially expressed genes (DEGs) in octoploid strawberry (Benihoppe). Phylogenetic relationship of proteins associated with signalling pathways in strawberry. Numbers at the branches indicate posterior probabilities and bootstrap percentages based on 1000 replicates. Heatmap was generated using the average values [$\log_{10}(\text{FPKM}+1)$] of three biological samples per treatment, representing the relative transcript expression levels of DEGs in leaves. The colour bar indicates the expression values as an increasing intensity gradient (blue, low expression; red, high expression).

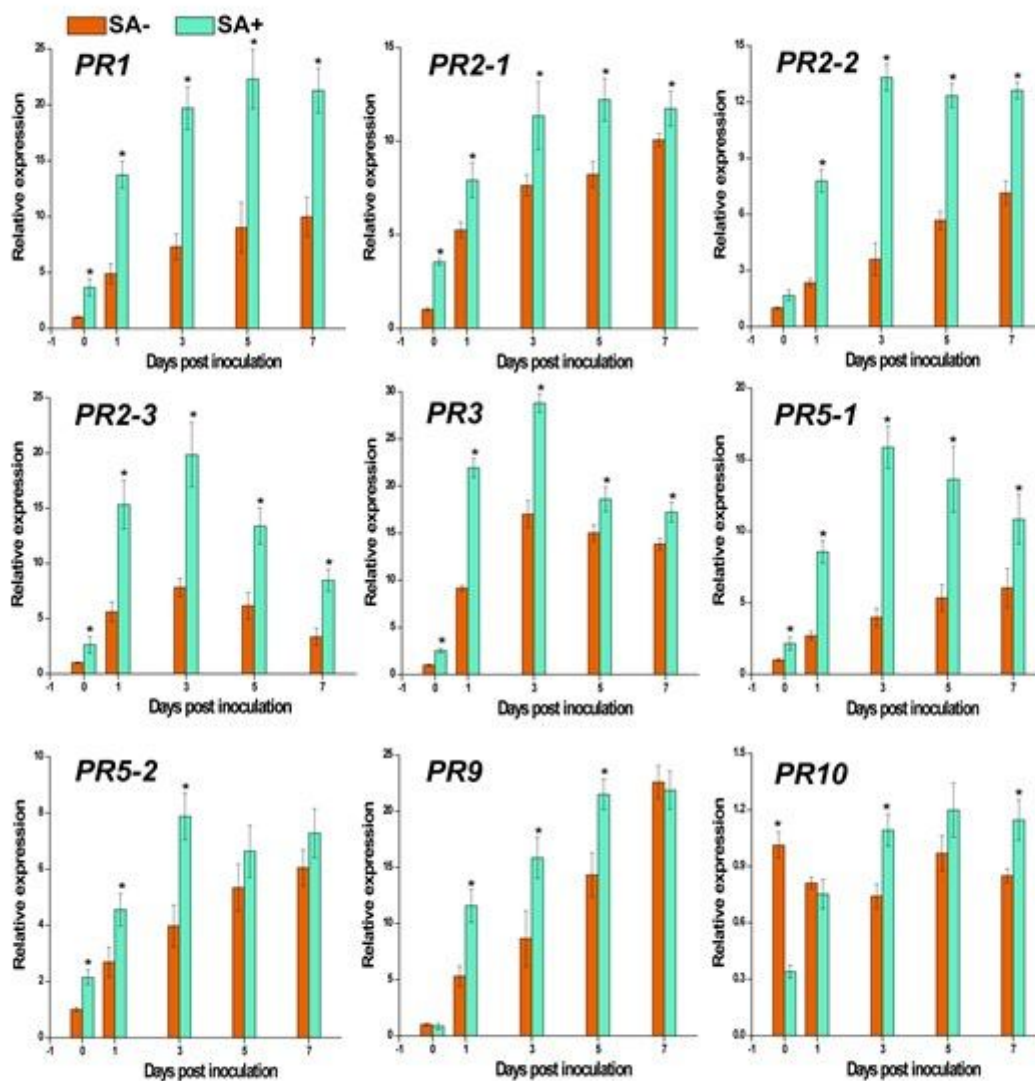


Figure 4

Effect of SA and *P. aphanis* infection on the expression of pathogenesis-related (PR) genes in strawberry leaves with (SA+) or without (SA-) treatment with SA at different time points after inoculation. Two actin genes were used as reporter genes, and the values were normalised to the non-inoculated untreated control. Data are expressed as the mean \pm SD of three biological replicates. An * above the bar indicates statistically significant differences between groups at the same time point.

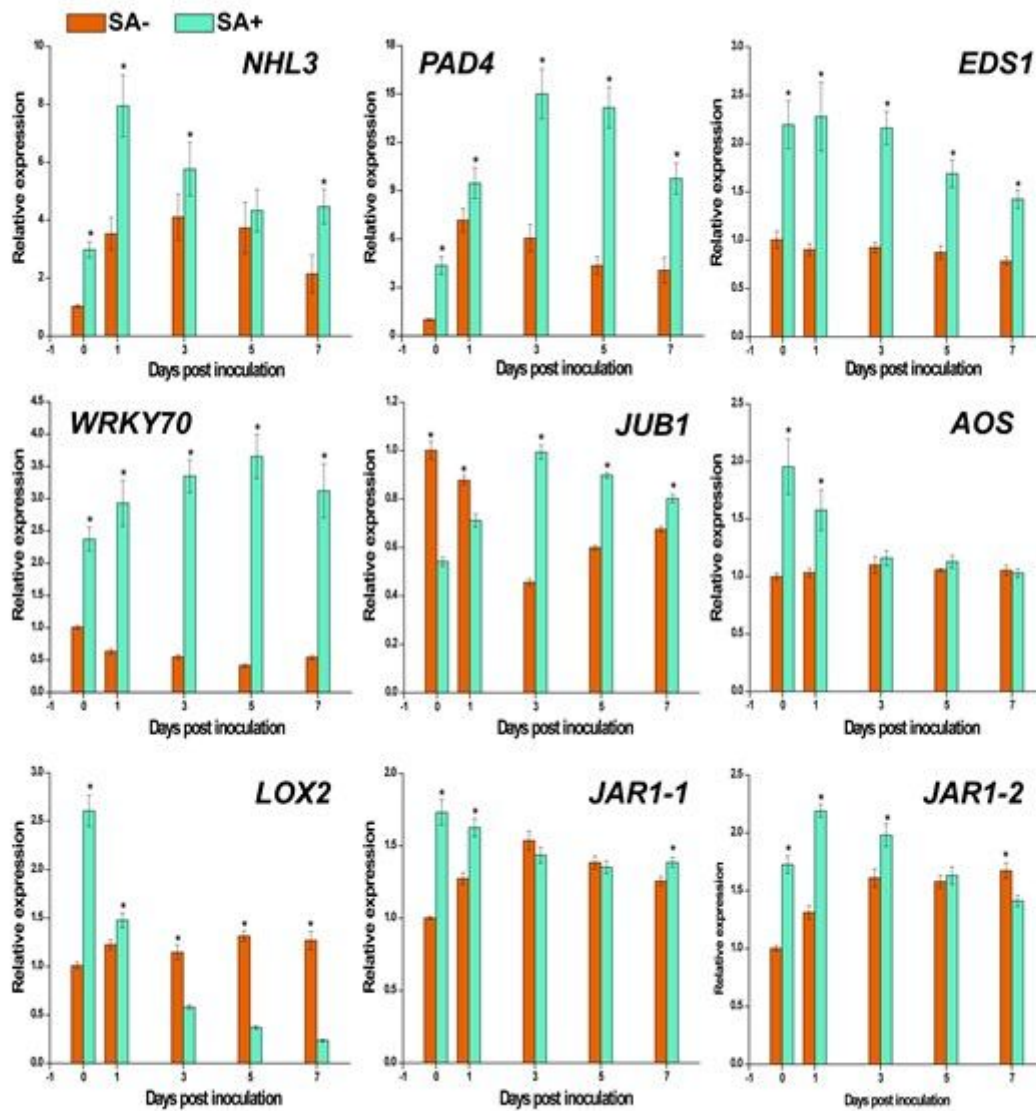


Figure 5

Effect of *P. aphans* infection on the expression of plant SA transduction factors in strawberry leaves with (SA+) or without (SA-) treatment with SA at different time points after inoculation. Two actin genes were used as reporter genes, and the values were normalised to the non-inoculated untreated control (Control-). Data are expressed as the mean \pm SD of three biological replicates. An * above the bar indicates statistically significant differences between groups at the same time point ($P < 0.05$).

- S1.jpg
- supplementarytable.xlsx
- S3.jpg
- S2.jpg